Macromolecules

Volume 15, Number 4 July–August 1982

Poly(7,16-dihydroheptacenes): A New Type of Obligate Ladder Polymer Conformationally Restricted to Two Dimensions

Vinod R. Sastri, Robert Schulman, and David C. Roberts*

Department of Chemistry, Rutgers, The State University of New Jersey, New Brunswick, New Jersey 08903. *Received February 16, 1981*

ABSTRACT: A monomer containing two anthracene units, 7,16-dihydroxy-7,16-bis(1-octynyl)-7,16-dihydroheptacene, was synthesized and caused to polymerize by irradiation with sunlight or its artificial equivalent. The polymerization was accompanied by the loss of the characteristic anthracene-like UV absorption of the monomer, implicating face-to-face dimerization of the anthracene units. The resulting mixtures of higher molecular weight substances were resolved by precipitation fractionation. The major and highest molecular weight component, with apparent $\bar{M}_n$(GPC) = 5600 and spread over the range 1000–12 000, was purified to homogeneity and characterized with regard to its spectroscopic properties, viscosity, exclusion behavior, and thermal stability. The results are consistent with the formulation of the polymer as a semirigid ladder, which is confined locally to two dimensions as a consequence of the rigidity of the dianthracene units.

In the course of planning efficient routes to large rigid macrocycles composed of fused rings, it became evident to us that such molecules might be obtained in good yield as byproducts from the polymerization of suitably designed monomer molecules, especially if the resulting oligomers were restricted conformationally in such a way that the reactive ends were constrained to exist only within a single plane. It further became apparent that polymers resulting from such systems, which might be called "two-dimensional polymers", might be of interest themselves, by virtue of these conformational restrictions.

Two-Dimensional Polymers. One can visualize two distinct ways to restrict polymer growth locally to two dimensions. One possibility consists of chains of fused planar rings, such as A, which resist twisting out of the

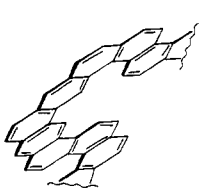

A

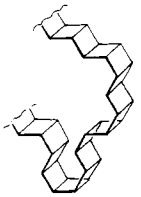

B

plane of the atoms because it leads to a decrease in π overlap. The other possibility consists of chains of fused rings which are bisected by a common plane of symmetry (such as B), and where resistance to twisting out of this plane results from the inherent rigidity of the fused-ring units in the polymer.

Polymers of type A have been reported in fair variety;[1] typically these are obtained by cyclopolycondensations of complementary comonomers, e.g., aromatic tetramines with aromatic bis(anhydrides), and consist of fused heterocyclic rings, although carbocyclic systems of this type are known.[2] These are perhaps better described as "one-dimensional" as a result of their essentially linear constitution. Large all-planar fused-ring macrocycles might be prepared by similar cocondensations involving angularly constituted monomers, but this appears to have been unexplored to date; in any case, their lack of flexibility within the plane would reduce the likelihood of cyclization.

Far more attractive for the latter purpose would be systems giving rise to polymers of type B. Varying degrees of flexibility within the plane of symmetry may be imparted to the chain without sacrificing resistance to twisting out of that plane, depending upon the particular arrangement of fused rings involved. This in-plane flexibility may enhance the probability that two reactive ends of an oligomer will meet, resulting in the formation of novel fused-ring macrocycles; furthermore, it may impart a wide range of unusual and desirable physical properties to the polymers themselves, in contrast to known examples of polymers of type A, which are invariably brittle and insoluble due to their extreme rigidity.

Our research has therefore centered on development of systems expected to yield two-dimensional polymers of type B, which are at present almost entirely unexplored. Known examples of polymers of this type are limited to Diels–Alder oligomers of cyclopentadiene and 1,3-cyclohexadiene, which are reported not to have exceeded the hexamer stage.[3] Higher molecular weight Diels–Alder copolymers of benzoquinone with 1,2-dimethylenecyclobutane and 1,2,4,5-tetramethylenecyclohexane,[3] which might superficially appear to be examples of type B

0024-9297/82/2215-0939$01.25/0

polymers, can be seen from analysis of Dreiding models to be subject to a surprising degree of flexibility out of the plane of symmetry and therefore not to be true members of this class.

Other so-called "ladder" polymers, which might superficially appear to satisfy the requirements of a type B polymer, are formed by two-step ring-forming reactions, in which any interference with the second (cyclization) step (e.g., an intermolecular condensation) results in a flaw in the ladder constitution. Even a very small proportion of such flaws can be expected to have a large effect on the polymer's properties. Only a polymer formed via a one-step cyclization process (viz., a cycloaddition reaction) can have an obligate ladder structure.

Constraints on Monomer Structure. Preparation of polymers of type B requires a monomer that (a) bears two mutually reactive functionalities that share a plane of symmetry, (b) polymerizes in a ring-forming process with maintenance of that plane of symmetry in the newly formed rings, and (c) gives rise to a system of fused rings that is resistant to twisting out of that plane of symmetry. A fourth requirement is necessary for the formation of the originally sought cyclic oligomers, viz., (d) the two ends of the growing polymer chain must bear the same mutually reactive functionalities as does the monomer. A pair of complementary comonomers would work equally well if their 1:1 adduct were to meet the same constraints as those for the single bifunctional monomer. The simplest way of satisfying these criteria is to make use of cycloaddition as the crucial reaction and to arrange the components in the monomer so as to be bisected by the same plane of symmetry.

All the aforementioned criteria are met by the monomer described herein, 7,16-bis(1-octynyl)-7,16-dihydroheptacene-7,16-diol (1), which can be induced to polym-

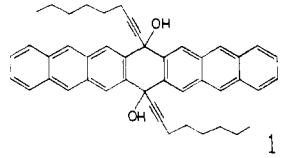

1

erize photochemically by face-to-face dimerization of its anthracene units. Previous work on polymerizations based on anthracene photodimerization[4,5] provides useful data with which we may compare our results. We now present evidence that the resulting polymer has the expected part-structures **2a** and/or **2b**, and thus constitutes the first unambiguous example of a two-dimensional polymer of the second type.

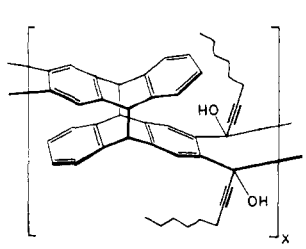

2a

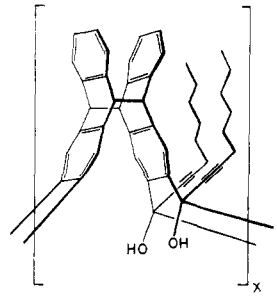

2b

It appears that the Diels–Alder reaction may also be applied successfully to the preparation of type B polymers. We have obtained favorable preliminary results for the thermal Diels–Alder copolymerization of 1 with *p*-benzoquinone, to provide polymers of generalized structure 3; their properties will be reported in detail in a subsequent article.

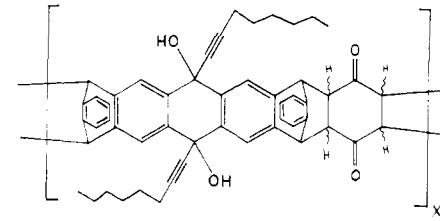

3

Abbreviations. The following abbreviations are used throughout this paper: $\bar{M}_n$ and $\bar{M}_w$, number- and weight-average molecular weight; $\bar{DP}_n$ and $\bar{DP}_w$, number- and weight-average degree of polymerization (chain length); GPC, gel permeation chromatography; TGA, thermogravimetric analysis; MWD, molecular weight distribution.

Experimental Section

A. Materials. 7,16-Bis(1-octynyl)-7,16-dihydroheptacene-7,16-diol (1). 1-Octyne[6] (12.4 mL) in 50 mL of hexane (distilled from Na), deaerated by flushing with a stream of dry nitrogen, was stirred under positive nitrogen pressure and treated with 64 mL of 1.65 M methyllithium in hexane (Lithium Corp. of America). Sufficient THF (distilled from $LiAlH_4$) was added to dissolve the initially formed precipitate. The resulting solution was transferred via cannula to a flask containing a stirred, nitrogen-flushed suspension of 8.65 g of heptacene-7,16-quinone[7] in 50 mL of dry hexane. After 24 h of refluxing, a clear, deep red solution was obtained, and this was diluted with several volumes of dry ether and washed once with saturated aqueous NH_4Cl and twice with water. The organic phase was dried over anhydrous Na_2SO_4 and concentrated in vacuo. The residue was purified by chromatography on a short column of Fisher activated alumina (neutral), using 3:2 EtOAc–ether to elute the product as a yellow band. Concentration and recrystallization from CCl_4 afforded 8.27 g (62%) of yellow crystals, mp 184–186 °C. Spectral data are reported in Table I. Anal. Calcd for $C_{46}H_{44}O_2$: C, 87.86; H, 7.05. Found: C, 87.59; H, 7.18.

Photopolymerization of Monomer 1. Poly[7,16-dihydroxy-7,16-bis(1-octynyl)-5,7,9,14,16,18-hexahydroheptacene-5,18:9,14-tetrayl] (2). In a typical preparation, monomer 1 (0.2915 g) was dissolved in 33.7 mL of THF (distilled from $LiAlH_4$) in a 100-mL quartz round-bottomed flask containing a magnetic stirring bar. The solution was degassed by four vacuum freeze–thaw cycles, the flask was vented with nitrogen, and then the solution was irradiated with a GE 275-W sunlamp (ventilated by forced-air cooling) under positive nitrogen pressure with constant stirring. During this time the solution turned from light yellow to light orange, and the characteristic anthracene-like absorption of the monomer at 277 nm was lost. After 48 h of irradiation, no further changes in the UV spectrum were observed. The solution was concentrated under reduced pressure to 6 mL and subjected to a solvent fractionation procedure, involving partial precipitation of polymer by addition of an aliquot of methanol, followed by immediate centrifugation and washing of the precipitate with methanol. The details of the procedure, yields, and average molecular weight values of fractions are reported in Figure 1. The major polymeric component, designated 2-S1, obtained in 51.5% yield, had the following physical parameters: apparent $\bar{M}_n$ = 5600, apparent $\bar{M}_w$ = 15000, apparent $\bar{M}_z$ = 34400, H (dispersity) = 2.69, $[\eta]_{THF}^{25}$ (capillary) = 0.0662 dL/g. Spectral data for 2-S1 are compared in Table I to data for related substances. The polymer is very soluble in the solvents tetrahydrofuran, toluene, chloroform, carbon tetrachloride, acetone, and diethyl ether. It is insoluble in methanol, ethanol, pentane, and hexane. It forms stable films on evaporation of its solutions.

Preparation of the Anthracene Adduct of 1 (Model Compound 4). Monomer 1 (0.2519 g (0.4 mmol)) and anthracene (0.3005 g (1.69 mmol)) (MCB) were dissolved in 30 mL of freshly distilled THF in a 100-mL quartz round-bottomed flask, and the

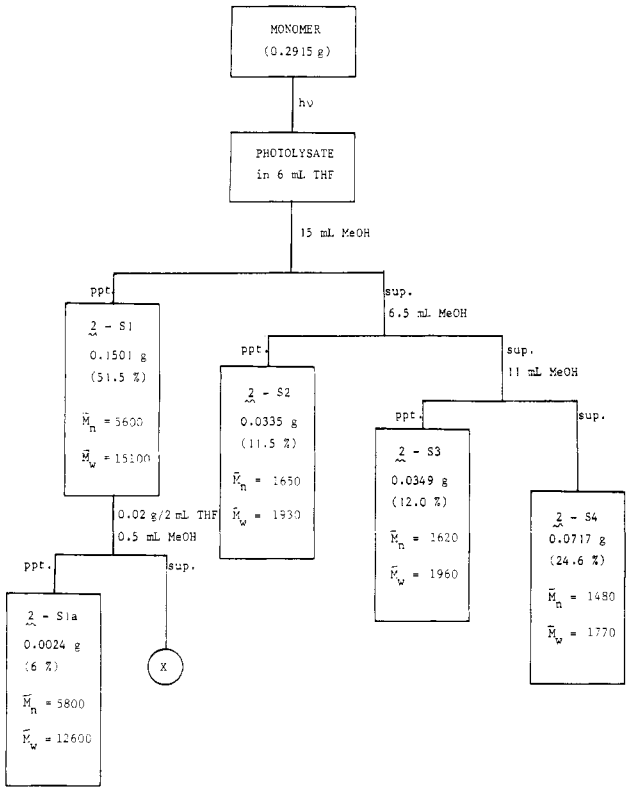

Figure 1. Flow diagram for precipitation fractionation procedure.

stirred solution was freeze degassed four times and irradiated under positive nitrogen pressure with an air-cooled GE 275-W sunlamp. A white precipitate began to form after about 12 h; irradiation was continued for a total of 24 h. The precipitate was then filtered (it was found to be anthracene dimer) and the filtrate was concentrated to 15 mL, filtered again, and finally concentrated to 2 mL. This crude mixture was subjected to preparative TLC on a freshly opened Whatman PLK5F plate, using 4:1 petroleum ether (B)–ether as eluent; the band at $R_f \sim 0.5$, constituting the major component, was removed and extracted with THF, affording on evaporation 0.0425 g of yellowish amorphous powder, mp 144–148 °C, which was shown by TLC analysis to be homogeneous and distinct from monomer 1, anthracene, and anthracene dimer. Yield (calcd for 1:1 adduct), 13.2%. Spectral data are reported in Table I.

B. Polymer Characterization. Gel Permeation Chromatography. Unless otherwise noted, a Waters Model 6000A liquid chromatograph, equipped with two E-linear Bondagel columns in series and a Waters Model 730 data module, was employed. UV absorption at 254 nm was monitored, and the following standard conditions were routinely employed: Solvent, tetrahydrofuran (Waters HPLC grade); pressure, 1500 psi; flow rate, 0.9 mL/min. Samples of polystyrene molecular weight standards, assayed at MW values of 50 000, 8500, 4000, and 1800, were obtained from Waters and employed for the studies described herein.

After the system had reached a steady state, it was calibrated for a linear fit of number-average molecular weight vs. elution volume using the four standard polystyrene samples. The data module was programmed to treat about 50 slices of equal elution volume over the molecular weight range of the sample, and from the data so obtained, it directly calculated apparent number- and weight-average molecular weight values (referred to in this paper as $\bar{M}_n$(app) and $\bar{M}_w$(app), respectively), as follows:

$$\bar{M}_n(\text{app}) \equiv \sum_i A_i / \sum_i (A_i/M_i) \quad (1)$$

$$\bar{M}_w(\text{app}) \equiv \sum_i (M_i A_i) / \sum_i A_i \quad (2)$$

where A_i and M_i are absorbance (254 nm) and extrapolated molecular weight values, respectively, for slice i. Apparent $\bar{D}\bar{P}_n$ and $\bar{D}\bar{P}_w$ values are obtained by dividing these numbers by the monomer molecular weight (629).

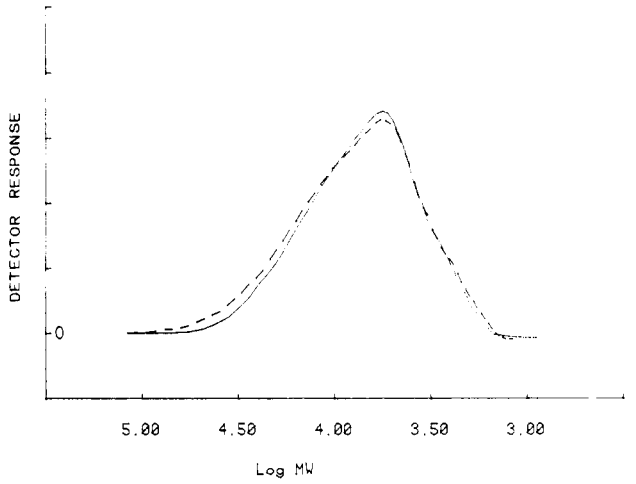

Figure 2. GPC elution profile of polymer fraction 2-S1. Molecular weight scale is based on elution volumes of polystyrene standards. Solid line, UV absorbance at 254 nm; broken line, relative refractive index.

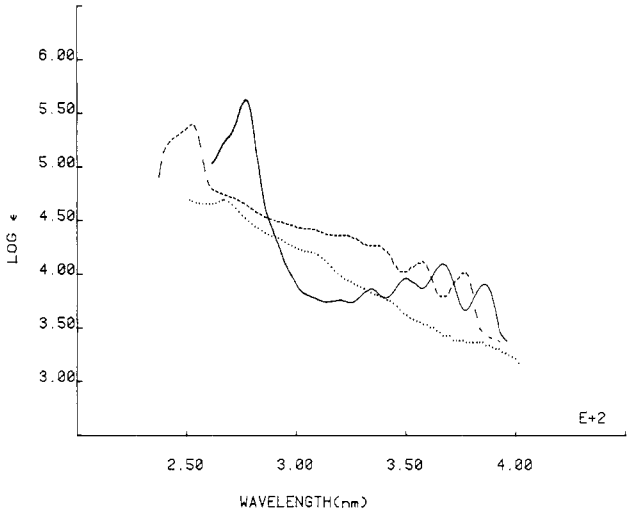

Figure 3. Optical absorption spectra. Solid line, monomer 1; dashed line, model compound 4; dotted line, polymer fraction 2-S1. Values of for the polymer were based on monomer molecular weight.

GPC Fractionation of Polymer 2-S1. Fractions 2-G1 to 2-G9. Polymer 2-S1 (0.01 g) was dissolved in 1 mL of THF. Twenty-five-microliter samples were injected into the chromatography system, and fractions were collected for each run at intervals of 15 s (flow, 0.9 mL/min). This was repeated until the entire sample had been subjected to the procedure. The elution profile is shown in Figure 2. The fractions were individually characterized by GPC by dissolving each in 0.5 mL of THF and injecting 0.5-μL samples. Results are displayed in Table II.

General Spectroscopy. Details of spectroscopy are given along with results in Table I. Infrared spectra were obtained on a Perkin-Elmer 727-B spectrophotometer. Ultraviolet spectra were obtained on solutions in spectrograde THF in a 1-cm cell, employing a Cary 17D spectrophotometer, over a range of 500–240 nm (Hg and W sources). They appear graphically in Figure 3. NMR spectra were recorded on a Varian CFT-20 spectrometer at 80 MHz (^{1}H) or 20 MHz (^{13}C), using $CDCl_3$ as solvent in all cases.

Fluorescence Data. Spectra were recorded on a Perkin-Elmer MPF-3L fluorescence spectrophotometer interfaced to a digital plotter. A 1-cm cell was used, and spectrograde chloroform was used as solvent. Both slits were maintained at 6 nm. Emission spectra were obtained with an excitation wavelength of 335 nm (found to give maximal emission for polymer solutions; the spectra were relatively unaffected by the choice of wavelength). Excitation spectra were obtained with both 420- and 480-nm emission monitoring. Fluorescence data for the narrow-molecular-weight

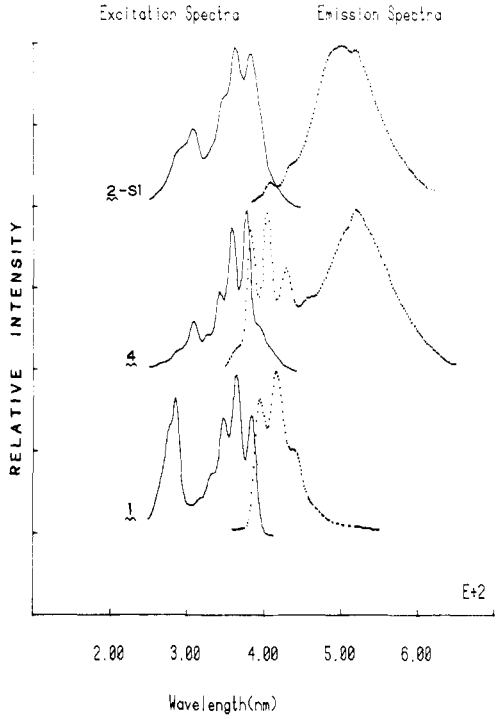

Figure 4. Fluorescence spectra of **1**, **2-S1**, and **4**. Excitation spectra were obtained by monitoring emission at 420 nm; emission spectra were obtained with excitation at 335 nm.

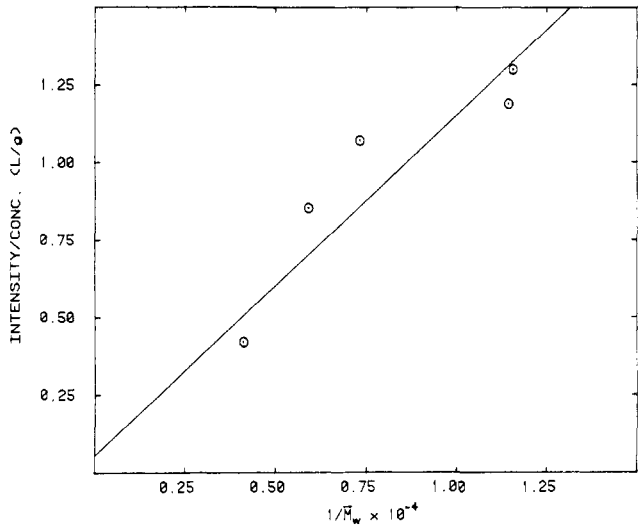

Figure 5. Molecular weight dependence of fluorescence intensity for polymer fractions **2-G1** to **2-G5**. The correlation line includes a point at (0,0). Excitation wavelength, 335 nm; emission wavelength, 520 nm.

range fractions (**2-G**) are given in Table II; other data are found in Figures 4 and 5.

Thermogravimetric Analysis. A Mettler Model TA-1 vacuum thermoanalyzer was employed. The finely ground sample was heated in vacuo at a rate of 6 °C/min. Results for polymer **2-S1** and model compound **4** are as follows:

	2-S1	4
wt loss range	155–175 °C	180–245 °C
% wt loss	12.0 ± 0.5%	45 ± 1%
% octynyl moieties lost from 2	34%	
% anthracene and/or octynyl groups lost from 4		89%

Vacuum Thermolysis of Polymer 2. Fraction **2-S1** (0.5021 g) was placed in a 25-mL round-bottomed flask equipped with a short-path distilling head and receiving flask. The entire apparatus was evacuated with a mechanical pump and the receiving

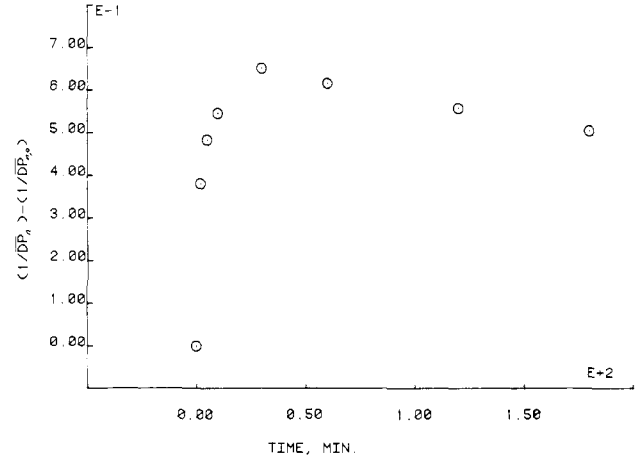

Figure 6. Solution-phase thermal degradation of **2-S1** at 180 °C.

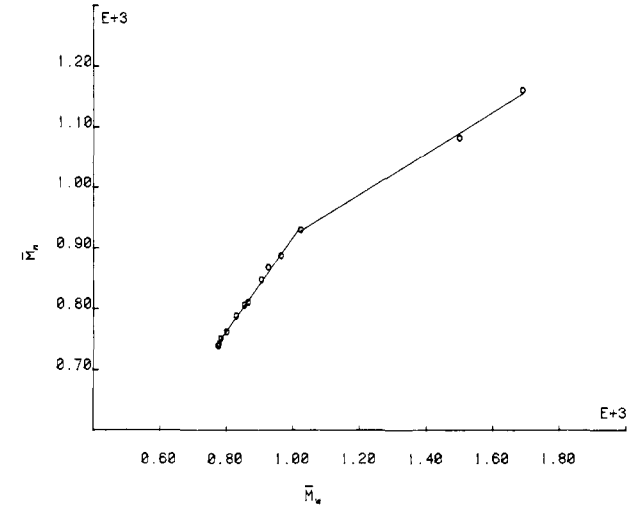

Figure 7. GPC monitoring of photopolymerization of **1**. The two solid lines are least-squares fits of the points within their spans.

flask was cooled in liquid nitrogen. The flask containing the polymer was heated with a thermostated oil bath, initially at 180 °C, followed by a gradual increase in temperature to 250 °C. At about 180 °C, the polymer began visibly degrading, eventually becoming a charred brown-black mass. The distillate was analyzed by gas chromatography (24-ft HIPAK/SE-30, 75 °C) and appeared to consist almost entirely of one component. This was collected and subjected to GC–mass spectroscopy, where it exhibited a spectrum nearly identical with that for 1-octyne (obtained from the NIH-EPA mass spectral data base).

Solution-Phase Thermal Decomposition of Polymer 2. Polymer, fraction **2-S1** (0.01 g), was dissolved in 10 mL of distilled triglyme (Aldrich, bp 216 °C), and 1 mL was pipetted into each of eight ampules. The solutions were individually freeze degassed (four cycles) and the ampules sealed under positive nitrogen pressure. They were immersed in a thermostated oil bath maintained at 180 ± 5 °C for various lengths of time and then cooled immediately to room temperature, and the contents were subjected to molecular weight analysis by GPC (0.2-μL samples). The data were treated as described by Jellinek[8] for random chain scission and plotted in Figure 6.

C. Photopolymerization Studies. Molecular Weight Distribution Monitoring during Irradiation. Monomer **1** (0.0224 g) was dissolved in 20 mL of THF, freeze degassed four times, and irradiated under nitrogen in a quartz round-bottomed flask equipped with a rubber septum (GE 275-W sunlamp). Periodically an aliquot of solution was removed by syringe, and a 0.2-μL sample was subjected to GPC analysis using the system described. The results are given in Figure 7.

Effect of Initial Monomer Concentration of Polymerization. Samples of monomer **1** in distilled THF (made up to a volume of 30 mL) of varying concentrations were treated as above,

Table I
Spectral Data for Monomer, Polymer, and Model Compounds

	1	2-S1	4	anthracene photodimer	anthracene[a]
IR: ν, cm^{-1}	3355, 3475	3370	3400		
	2215	2220	2220		
	1621		1620		1620
		1600	1590	1600	
		1480	1470	1470	
	1460[b]	1460[b]	1450[b]	1450[c]	1450[c]
UV: λ_{max}, nm (log ϵ)				212[d] (4.30)	
				250[e] (3.50)	
	277 (5.61)	267.9 (4.74)[f]	254.4 (5.40)[g]		250 (5.30)
			272.8 sh (4.67)[g]	270 sh[d] (3.00)	
		306.4 sh (4.23)[f]	306.4 (4.35)[g]	312 sh[e] (2.50)	
	315.8 (3.69)				
	331.2 (3.85)		323.4 (3.86)[g]		322 (4.14)
	347.7 (4.03)		339.9 (3.91)[g]		338 (4.42)
	365.4 (4.12)		361.6 (4.19)[g]		355 (4.59)
	385.1 (3.92)	385.1[h] (3.50)[f]	372.9 (4.14)[g]		376 (4.58)
^{13}C NMR: δ ($CDCl_3$) vs. $CHCl_3$ at δ 77.00	136.16	143.7			
	132.16	142.8 (unresolved)			
	131.03	137.5			131.5 (C-1a)
	128.07 aromatic C's				
	126.69	127.9			127.9 (C-1)
	125.73	127.3 (unresolved)			126.0 (C-9)
	125.56	125.8			125.1 (C-2)
	90.02	91.1			
	82.36 quaternary C's	83.1			
	69.86	67.8			
		53.58 (methine)			
	31.23	31.39			
	28.70				
	28.36 aliphatic C's	28.76 (unresolved)			
	22.45	22.66			
	18.99	19.01			
	13.95	14.07			
^1H NMR: δ ($CDCl_3$) vs. Me_4Si	8.68 (4 H, s)				
		7.72-8.68 (2.07 H)			
	8.43 (4 H, s)		8.35 (2 H, s)		
	7.97 (4 H, dd)	7.18-7.72 (2.26 H)	7.70-8.20 (4 H, m)		
	7.40 (4 H, dd)	6.31-7.18 (4.80 H)	7.25-7.45 (8 H, m)		
		6.05 (0.68 H)	6.4-7.0 (8 H, bm)		
		5.55			
	4.68 (2 H, s)	4.62 (2 H, s)	4.54 (2 H, m)		
		3.25-4.38 (1.3 H)	3.5-3.8 (scattered, <2 H)		
	2.38 (4 H, t)		2.65 (4 H, bs)		
	1.28-1.53 (16 H)	0.45-2.95 (26 H, b)[i]	0.6-2.25 (26 H, b)		
	0.73-0.93 (6 H)				

[a] Sources of IR and UV data: "Sadtler Handbooks of Infrared and Ultraviolet Spectra", Simons, W. W., Ed.; Sadtler Laboratories: Philadelphia, Pa., 1978. [b] Film (NaCl plate). [c] KBr pellet. [d] Reference 14. [e] Reference 15. [f] ϵ values based on monomer molecular weight (628.86). [g] ϵ values based on monomer + 1 anthracene (807.09). [h] Not a λ_{max}. [i] Spectrum essentially unchanged at 55 °C.

Table II
Data on Narrow-Molecular-Weight Fractions 2-G1 to 2-G9

	wt,[a] g	$\bar{M}_n$(app)	$\bar{M}_w$(app)	fluorescence I_{520}/concn	wt absorpt (254 nm), L/g
2-G1	0.0006	11500	24200	0.416	1.3
2-G2	0.0008	9500	17000	0.853	2.8
2-G3	0.0010	7550	13700	1.070	7.3
2-G4	0.0012	5050	8750	1.187	16.9
2-G5	0.0016	5150	8650	1.297	22.3
2-G6	0.0019	3300	5200	0.908	26.0
2-G7	0.0013	1850	3100	1.614	21.1
2-G8	0.0009	1000	1800	1.500	18.8
2-G9	0.0006	1000	1400	0.600	6.6

[a] Total 0.0099.

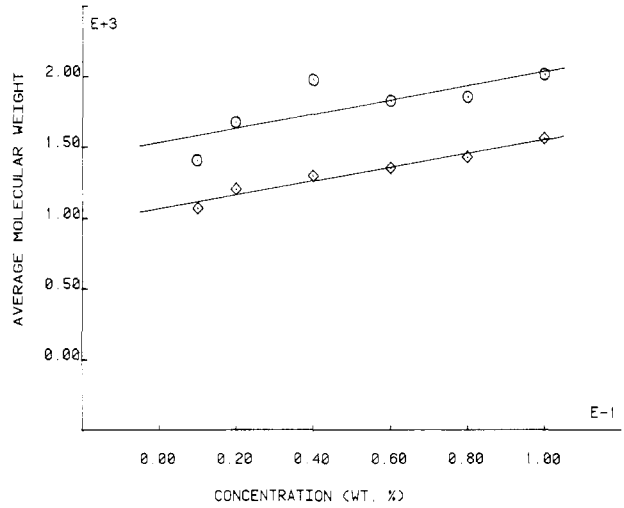

Figure 8. Effect of initial monomer concentration on ultimate average molecular weight of polymer. Upper points represent $\bar{M}_w$(app) values and lower points represent $\bar{M}_n$(app) values.

irradiating each sample until all UV absorption due to monomer had disappeared. The solutions were concentrated to ~1 mL and they were subjected to GPC analysis using the system described. The results are shown in Figure 8.

Results and Discussion

The synthesis of monomer 1 from 7,16-heptacenequinone was the result of numerous attempts to prepare symmetrical bis(anthracenes) by addition of various organometallic reagents to the quinone, which is exceedingly insoluble in all solvents. Most such reactions afforded complex mixtures containing highly colored products, possibly resulting from conjugate addition of the organometal to the quinone or from processes involving electron transfer from the organometal to the quinone. Optimal results were obtained with a highly ionic or polarized reagent (a lithium acetylide) in a very nonpolar solvent (hexane), favoring the hard–hard interactions that lead to normal carbonyl addition. The long side chains were chosen to improve the solubility properties of the monomer and polymer.

The structure of 1 is confirmed by ^{1}H and ^{13}C NMR, IR, UV (see Table I), and elemental analysis; the relative stereochemistry of the substituents on the 7,16 positions has not been elucidated, although owing to its apparent spectroscopic and chromatographic homogeneity, it is probably a single isomer. By analogy to the behavior of pentacene-6,13-quinone toward phenyl Grignard (conclusively shown to afford trans product[9]), the trans structure is viewed as most likely for 1. Attempts to prepare a cyclic version of 1, which could exist only in the *cis*-diol form, by addition of dilithium salts of 1,5-hexadiyne and 1,7-octadiyne to the quinone were unsuccessful.

Characterization of polymer 2 was facilitated by a comparison of its spectral data with those of both monomer 1 and a model compound 4 prepared by irradiating 1 in the presence of excess anthracene. Model compound 4, although only partially characterized, is formulated as a monoanthracene adduct, owing to unambiguous UV and fluorescence data indicating the presence of an anthracene chromophore. NMR and IR data are reasonably consistent with this formulation (see Table I).

The most revealing IR and NMR spectral changes that occur in going from the monomer to the polymer are (1) loss of the characteristic 1620-cm^{-1} aromatic ring stretch associated with the anthracene system and its replacement by a band at about 1600 cm^{-1} (the latter is found also in durene and is probably characteristic of a 1,2,4,5-tetrasubstituted benzene), (2) replacement of a single band at 1460 cm^{-1} with a doublet at 1460 and 1480 cm^{-1} (a similar change has been observed in polymerization of other bis(anthracene) monomers[4a]—the doublet is characteristic of the anthracene dimer system), (3) loss of sharp anthracene NMR singlets at δ 8.68 and 8.43, with appearance of bridgehead absorptions at δ 3.25–4.38 (as compared to δ 3.70 and 4.20 for an analogous system,[4a] and (4) appearance of a carbon at δ 53.58 in the ^{13}C NMR spectrum of the polymer, which agrees well with a chemical shift of δ 50.4 reported for the bridgehead carbon of norbornadiene.[10] The model compound 4 exhibits features of both monomer and polymer; its ^{1}H NMR spectrum shows only two of the four uncoupled anthracene protons, the others possibly buried upfield due to ring current effects. Marked upfield shifts of aromatic protons are seen in the polymer ^{1}H NMR spectrum, which was considerably broadened overall. All these data strongly support the formulation of the polymer as 2.

Considerable difficulty was encountered in the interpretation of molecular weight data for polymer 2. It must be emphasized that all values reported herein for apparent $\bar{M}_n$, $\bar{M}_w$, $\bar{D}\bar{P}_n$, and $\bar{D}\bar{P}_w$ are, of necessity, relative and not absolute values, as they are based upon the viscosity/molecular weight relationship of the polystyrene molecular weight standards. However, two pieces of evidence lend some validity, in an absolute sense, to the numbers reported here. First, the monomer (M = 629), which itself is quite rigid, upon GPC analysis in this system afforded $\bar{M}_n$ = 637 ± 50. Second, the extinction coefficient of the 268-nm UV band of the polymer comes very close to that calculated from its apparent $\bar{D}\bar{P}_n$ based on GPC (vide infra).

A second, and more serious, problem stems from the uncertain relationship between molecular weight and extinction coefficient in the polymer presently under discussion. For polymers of the usual type (e.g., polystyrene) in which the number of chromophores is proportional to molecular weight, it is assumed that the absorbance A_i due

to any fraction i of the polymer is proportional to the weight of that fraction W_i per unit solution volume V, or

$$A_i = KW_i/V \tag{3}$$

where K and V are invariant over all i. On the basis of this assumption, we can derive from the definitions of $\bar{M}_n$(app) and $\bar{M}_w$(app) given in the experimental section (eq 1 and 2) the conclusion that these values in fact correspond to true number- and weight-average molecular weight values:

$$\bar{M}_n(\text{app}) = \frac{\sum_i \left(\frac{K}{V} W_i\right)}{\sum_i \left(\frac{K}{V}\frac{W_i}{M_i}\right)} = \frac{\sum_i W_i}{\sum_i \left(\frac{W_i}{M_i}\right)} = \bar{M}_n(\text{actual}) \tag{4}$$

$$\bar{M}_w(\text{app}) = \frac{\sum_i \left(M_i \frac{K}{V} W_i\right)}{\sum_i \left(\frac{K}{V} W_i\right)} = \frac{\sum_i (M_i W_i)}{\sum_i W_i} = \bar{M}_w(\text{actual}) \tag{5}$$

A different situation will hold for other types of polymers. In the case of structure **2**, where, at least for relatively low degrees of polymerization, the anthracene chromophores at the ends will dominate the UV absorption, the polymer will absorb proportionally less as molecular weight increases:

$$A_i = \frac{K}{V}\frac{W_i}{M_i} \tag{6a}$$

or

$$\log A_i = \log \frac{KW_i}{V} - \log M_i \tag{6b}$$

Under such circumstances, the $\bar{M}_n$(app) and $\bar{M}_w$(app) values must be interpreted differently:

$$\bar{M}_w(\text{app}) = \frac{\sum_i \left(M_i \frac{K}{V}\frac{W_i}{M_i}\right)}{\sum_i \left(\frac{K}{V}\frac{W_i}{M_i}\right)} = \frac{\sum_i W_i}{\sum_i \left(\frac{W_i}{M_i}\right)} = \bar{M}_n(\text{actual}) \tag{7}$$

Similarly, $\bar{M}_z$(app) can be interpreted as $\bar{M}_w$(actual). $\bar{M}_n$(app) takes on a deflated value which may have no physical significance:

$$\bar{M}_n(\text{app}) = \frac{\sum_i \left(\frac{K}{V}\frac{W_i}{M_i}\right)}{\sum_i \left(\frac{K}{V}\frac{W_i}{M_i^2}\right)} = \frac{\sum_i \left(\frac{W_i}{M_i}\right)}{\sum_i \left(\frac{W_i}{M_i^2}\right)} = ? \tag{8}$$

In order to determine the extent to which the polymer (fraction **2**-S1) was behaving according to eq 6, it was necessary to subject it to preparative fractionation by GPC. This provided nine fractions (referred to as **2**-G1 to **2**-G9) whose weights, apparent molecular weight distributions, fluorescence spectra, and absorptivity by weight (254 nm) were determined (see Table II). The latter values are plotted in Figure 9, where it can be seen that, at least at higher $\bar{M}_n$(app), log (absorptivity) drops off linearly with increasing log ($\bar{M}_n$). The slope is greater in magnitude than the value of −1 predicted by eq 6, which may simply reflect the fact that the $\bar{M}_n$(app) values are deflated according to eq 8. It may also be noted that the $\bar{M}_n$ and $\bar{M}_w$ values calculated from the $\bar{M}_w$(app) data on the "G" fractions are

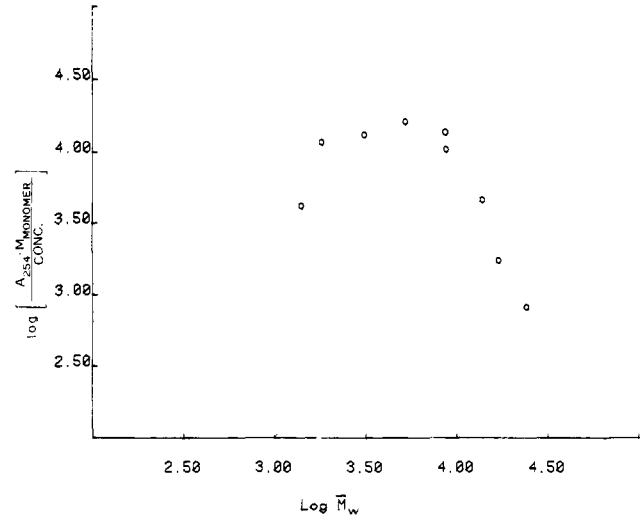

Figure 9. Molar absorptivity (based on monomer molecular weight) of polymer fractions **2**-G1 to **2**-G9 as a function of $\bar{M}_w$(app).

Table III
Comparison of Molecular Weight Data Obtained by Different Means

	$\bar{M}_n$	$\bar{M}_w$
apparent (GPC with UV monitoring)	5600	15100
as calcd from $\bar{M}_w$(app) data in Table II	4500	8300
as calcd from $\bar{M}_w$(app) data from Table II, modified as described in text[a]	4800	21600

[a] Modified $\bar{M}_w$ data: **2**-G1, 148 500; **2**-G2, 68 900; **2**-G3, 26 300; **2**-G4, 11 400.

deflated related to those obtained directly for **2**-S1 (see Table III). This discrepancy, originally pointed out by a referee, led us to the initial recognition of the problem at hand. The similarity of shape between the UV and refractive index elution curves for the polymer "S" fractions (for example, see Figure 2) had initially led us to place confidence in the UV data.

We have arrived at a means of resolving this discrepancy based on the presumed validity of eq 6 at higher molecular weight values. (It might be reasoned that the lower molecular weight components remained as such during the polymerization due to partial loss of their anthracene functionalities, as discussed below.) $\bar{M}_w$ values for fractions **2**-G1 to **2**-G4 were inflated so as to give a modified plot analogous to Figure 9, but with a slope of −1 intersecting the point corresponding to **2**-G5. These new $\bar{M}_w$ values were used to calculate overall $\bar{M}_n$ and $\bar{M}_w$ values, which are given in Table III and which are more consistent with the "apparent" values obtained directly. It would probably be foolish to put any faith in the validity of these individual $\bar{M}_w$ values, but this exercise confirmed our interpretation of the "apparent" molecule weight averages as valid conservative estimates. All molecular weight data appearing in the figures are "apparent" values.

The optical spectra provide additional evidence in support of the proposed structures of **1**, **2**, and **4** (Figure 3). The monomer exhibits a red shift of 3900 cm^{-1} (vs. anthracene) in the short-wavelength band due to coupling of the two anthracene chromophores along their mutual long axis. This is diminished in the polymer and all but eliminated in the model compound, which contains a single chromophore. The long-wavelength bands exhibit considerably weaker coupling. The 268-nm band of the polymer has a log ϵ value of 4.74, which agrees well with the value of 4.66 calculated by assuming an apparent $\bar{DP}_n$ of 8.91 (based on molecular weight data),[11] and two red-

shifted anthracene chromophores plus internal durene and xylene units. The presence of anthracene units is clearly seen in the fluorescence excitation spectrum of **2**, even though they are essentially visible in the absorption spectrum (see Figure 4). All of the above observations lend strong support to the proposed structures **2**.

The model compound and all polymer fractions exhibit broad excimer-like fluorescence at 470–520 nm, with unperturbed anthracene fluorescence nearly absent in the polymer. The concentration and solvent dependence of the fluorescence behavior was typical for intermolecular excimer formation involving the anthracene end groups and argues strongly against electronic interactions of internal benzene chromophores as the source of this band. At very low concentrations in chloroform, a dissociated anthracene-like fluorescence band appeared in the spectra of the **2**-S1 fraction; the ratio of dissociated (420 nm, ϵ = 0) to excimer (495 nm, ϵ = 0) fluorescence was found to vary linearly with inverse concentration. Total suppression of excimer behavior was not possible, even at very low concentrations. In 1-chloronaphthalene as solvent (expected to solvate anthracene rings more favorably), excimer fluorescence was largely suppressed even at higher polymer concentrations, but spectral interference by solvent prevented good nonexcimer spectra from being obtained. The very strong tendency toward excimer formation in the polymer systems may be interpreted in several ways. One possibility is that a high degree of polymer aggregation may exist even in relatively good solvents such as chloroform. However, no irreproducibility in GPC results or nonlinearity in the capillary viscosity study was observed, possibly because aggregation is less favorable in THF. Alternatively, the lack of excimer fluorescence in the monomer may reflect a much more rapid rate of decay of the dissociated excited states (before excimers have a change to form) or preferential decay of the excimers, if any, by nonradiative processes such as the desired photodimerization reaction. It is likely that excimers involving polymer end groups will experience steric inhibition of photodimerization and therefore would be more easily observable by their fluorescence.

The assumption that excimer-like fluorescence behavior in the polymer is due to the interactions of anthracene end groups is further supported by fluorescence studies on individual narrow-molecular-weight range "G" fractions obtained by preparative GPC of the **2**-S1 polymer fraction. A fairly good inverse correlation of fluorescence intensity with molecular weight is observed in the fractions of higher molecular weight (see Figure 5), and this ceases to hold for the lower molecular weight fractions. A somewhat better correlation is obtained for $\bar{M}_w$(app) than for $\bar{M}_n$(app), which is in agreement with the expectation that for a polymer in which ϵ remains constant with increasing M, the $\bar{M}_w$(app) values will correspond to $\bar{M}_n$(actual) values (see above). Essentially all the fluorescence of these fractions was of the excimer type, and the spectra were all nearly identical in overall shape, so comparison of their relative intensities in this way was taken to be valid. It was not established that the polymer fractions all absorb with equal efficiency at the excitation wavelength (indeed, the absorptivity data (254 nm) in Table II would imply otherwise); this may account for the deviation from linearity observed.

The lower molecular weight G fractions exhibit considerably weaker fluorescence than expected (see Table II), indicating that some of the anthracene end groups in these fractions are not intact, due to either cyclic oligomer formation (discussed below) or side reactions (e.g., photo-

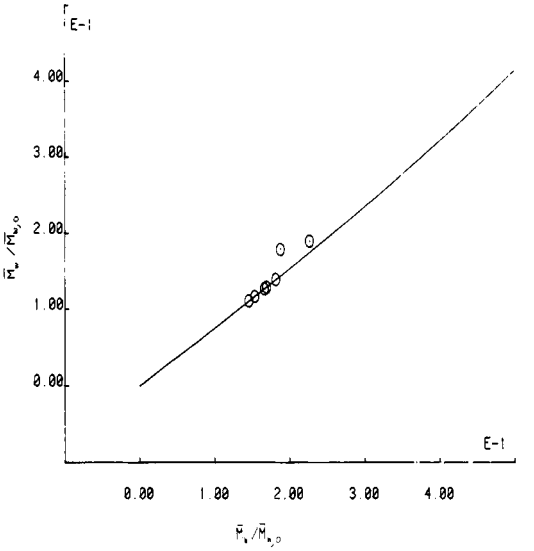

Figure 10. Scott plot[13] for solution-phase thermal degradation of **2**-S1. The solid line is the theoretical curve for a Schulz–Zimm MWD with initial H = 2.69 (obtained for **2**-S1 experimentally by GPC).

oxidation). These fluorescence intensities cannot be compared directly to that of the monomer, due to its lack of the excimer-like band. The isolation of pure individual oligomers, each bearing a pair of anthracene chromophores held in a well-defined relative geometry, would provide a unique system for investigating the nature of long-range energy transfer and electron-transfer processes.

The thermal stability of the polymer is relatively low, due both to the tendency for the alkynylcarbinol functionality to eliminate alkyne and regenerate a carbonyl group and to the tendency of the anthracene dimer units to undergo thermal cycloreversion, both of which were clearly seen in experimental studies and confirmed in the model compound. TGA studies, reflecting only loss of volatile groups, showed a solid-phase decomposition threshold temperature of 155 °C and a 12% weight loss; this was shown to be almost entirely due to loss of 1-octyne by GC–mass spectral characterization of volatilized products. The model compound decomposed at a somewhat higher temperature and to an extent possible only if both octyne and anthracene groups were lost. Anthracene dimer showed no decomposition until 225 °C. This trend seems logical in view of the additional steric crowding and mechanical stresses expected to bear on the dianthracene units in the polymer system.

Solution-phase thermal decomposition studies showed rapid depolymerization at 180 °C (loss of octynyl groups would have only minor effects on apparent molecular weight) as seen in Figure 6, with an apparent slow "reforming" process of unknown origin in competition. The first few points of this curve fit to an apparent initial cleavage rate constant of 0.35 min^{-1}, when treated according to Wall and co-workers.[12] Evidence supporting a random chain scission mechanism for the degradation was obtained by treating molecular weight distribution data at various stages of degradation as described by Scott,[13] assuming a Schulz–Zimm MWD (Figure 10). The nearly perfect agreement with the theoretical curve argues against the interesting possibility that electronically excited anthracene units generated by thermal chain cleavage might enhance the rate of cleavage of adjacent dianthracene units by some kind of energy-transfer process.

The photopolymerization of **1** with sunlight gave comparable results, except that the process was considerably slower (requiring roughly 2 weeks to effect nearly complete

destruction of the anthracene chromophore). Use of 254-nm light (Rayonet) gave a substantial amount of photoelimination of 1-octyne from 1 and a higher proportion of low-molecular-weight byproducts.

Some insight into the nature of the polymerization process was gained by studying the effect on polymer molecular weight distribution of both extent of polymerization and initial monomer concentration. Two distinct rate processes were noted in following the MWD during the polymerization process (Figure 7); initially, the product is nearly monodisperse and remains so until, at $M > 1000$, it begins to become increasingly polydisperse. This may reflect an initial rapid consumption of monomer to form dimers, followed by a slower (more sterically hindered) polymerization of dimers. The observation that ultimate polymer molecular weight depends on initial monomer concentration (Figure 8) probably results from an increased tendency of oligomers to undergo some (pseudo) first-order side reaction rather than polymerize further (second order) as their concentration decreases. The exact nature of this reaction is unknown, but it probably involves the destruction of anthracene chromophores, as these are observed to be present in deficient amounts in the lower molecular weight components of the polymer (see Table II).

Photooxidation due to traces of O_2, which remained in spite of careful degassing, and cyclization of oligomers by face-to-face anthracene photodimerization are possible competing reactions. The latter process is of special interest to us, owing to the unusual structure of the resulting fused-ring macrocycles, and constitutes the initial impetus that led us to carry out this study.

Acknowledgment. We thank Professors Ulrich Strauss and George Bird for enlightenment and encouragement, Professor Joseph San Filippo for mass spectral and vacuum TGA services, and Ms. Kathy Robison of Waters Associates for the generous loan of GPC equipment, which greatly facilitated this project. Primary support of this work by the Petroleum Research Fund, administered by the American Chemical Society, and additional assistance from the Rutgers Research Council and the Rutgers College School of Chemistry are gratefully acknowledged.

References and Notes

(1) For a recent review, see: Mark, H. F.; Atlas, S. M. *MTP Int. Rev. Sci., Org. Chem., Ser. Two* **1976**, *3*, 299–336.
(2) Stille, J. K.; Noren, G. K.; Green, L. *J. Polym. Sci., Part A-1* **1970**, *8*, 2245.
(3) Bailey, W. J.; Fetter, E. J.; Economy, J. *J. Org. Chem.* **1962**, *27*, 3479.
(4) (a) De Schryver, F. C.; Anand, L.; Smets, G.; Switten, J. *J. Polym. Sci., Polym. Lett. Ed.* **1971**, *9*, 777–780. (b) De Schryver, F. C.; Boens, N.; Put, J. *Adv. Photochem.* **1977**, *10*, 359–471.
(5) Tazuke, S.; Tanabe, T. *Macromolecules* **1979**, *12*, 848–853.
(6) Farchan Chemicals; redistilled before use.
(7) Ried, W.; Anthofer, F. *Angew. Chem.* **1954**, *66*, 604; obtained in 27% yield after exhaustive extraction with DMF.
(8) Jellinek, H. H. G. In "Aspects of Degradation and Stabilization of Polymers"; Jellinek, H. H. G., Ed.; Elsevier: Amsterdam, 1978; pp 1–38.
(9) Allen, C. F. H.; Bell, A. *J. Am. Chem. Soc.* **1942**, *64*, 1253–1260. More recently, cis products have been claimed (weak supporting evidence) for analogous reactions: Maulding, D. R.; Roberts, B. G. *J. Org. Chem.* **1969**, *34*, 1734–1736.
(10) Johnson, L. F.; Jankowski, W. C. "Carbon-13 NMR Spectra"; Wiley-Interscience: New York, 1972; No. 242. Similar chemical shifts are seen for various benzonorbornadiene derivatives.
(11) This value was calculated by the use of an expression based on the proposed polymer structure:

$$\log \epsilon = \log \left[\frac{2\epsilon_A + 2(\bar{D}\bar{P}_n - 1)(\epsilon_D + \epsilon_X)}{\bar{D}\bar{P}_n} \right]$$

where ϵ_A, ϵ_D, and ϵ_X are extinction coefficients at λ_{max} (from Sadtler Handbook) for anthracene at 250 nm (199 000), durene at 269 nm (269), and *o*-xylene at 269.5 nm (104). It is assumed for this calculation that λ_{max} for the anthracene end groups shifts to 268 nm but ϵ remains constant.
(12) Wall, L. A., et al. *J. Am. Chem. Soc.* **1954**, *76*, 3430. An assumption that the largest volatile chains contain 0.8 monomer unit (i.e., that monomer is being lost during the thermolysis) gave the best fit. Wall also adjusts this parameter to obtain good kinetic fits, although in neither case is there actual evidence of such volatilization.
(13) Scott, K. W. *J. Polym. Sci., Polym. Symp.* **1974**, *No. 6*, 321–344.
(14) Ferguson, J.; Mau, A.; Morris, J. M. *Aust. J. Chem.* **1973**, *26*, 91–102.
(15) Birks, J.; Appleyard, J.; Pope, R. *Photochem. Photobiol.* **1963**, *2*, 493–495.